

# IMPROVING CONTROL RELIABILITY AND QUALITY OF AIRCRAFT ENGINES BY MEANS THE SOFTWARE «VIRTUAL ENGINE»

F.D. Golberg\*, O.S. Gurevich\*, A.A Petukhov\*

\*Central Institute of Aviation Motors (CIAM), Moscow, Russia.

**Keywords:** *Automatic control system, onboard model*

## Abstract

*The mathematical tools and «virtual engine» software have been developed to be embedded into a digital automatic control systems of modern gas turbine engines (GTE) to use a new control method "intelligent engine" when variables which touch upon engine general performances, but are inaccessible to measurement, are directly controlled.*

## 1. Control philosophy and design concept of GTE control system in using onboard engine simulation model

At the present time, one of the most progressive directions of further gas turbine engines performances improving, both in Russia and abroad, is an intelligent GTE control by means of high-level onboard engine simulation models (OESM) which are built in the control system.

This is due to opportunity of using all-speed thermogasdynamical simulation models with continued possibilities of calculation in real time. It is caused by computational capability of on-board computers rising.

In this regard, research activities have been carrying out in CIAM, where all-speed transient models of various GTE types have been developed and improved for many years. The mathematical models, created by now, execute high-fidelity simulating of basic engine variables at all operation area and at steady and transient modes in their full range of variation, including start. At that, computational methods upon which calculation programs realizing such models were being ever-improving, thus, at the

present time, calculations on typical computers with the use of such models are executed in time that is much less than the real.

The use of such simulation models in GTE control systems permits conceptually change an engine control method by adoption of a control according to variables which touch upon general engine performances, but can not be measured: engine thrust  $R$  and specific fuel consumption  $C_R$ , gas temperature  $T_G^*$  at the inlet of HPT, compressors stall margin  $\Delta S_{Mi}$ , combustor air ratio  $\alpha_{CC}$  and many others.

At that, measurable variables which are traditionally used for an engine control and implicitly characterize an engine behavior (rotors speed  $n_i$ , LPT outlet temperature  $T_T^*$ , a complex of  $G_F/P_C^*$ , etc.) may be used for a backup basic control schedules and an engine protection.

Algorithmic software of control system containing full thermogasdynamical onboard engine simulation model and "virtual" control loops operating on variables calculated by onboard model was developed in the CIAM. Methods of OESM validation while in operation on a running engine were developed too.

A functional block-diagram of such control system that is developed for bypass turbofan engine (TFE) is shown in **Fig. 1**.

It contains controllers which act on the fuel flow  $G_F$  in the combustor chamber (CC), HPC guide vanes controllers, as well as air bleed valves of HPC and add stage (AS) controllers.

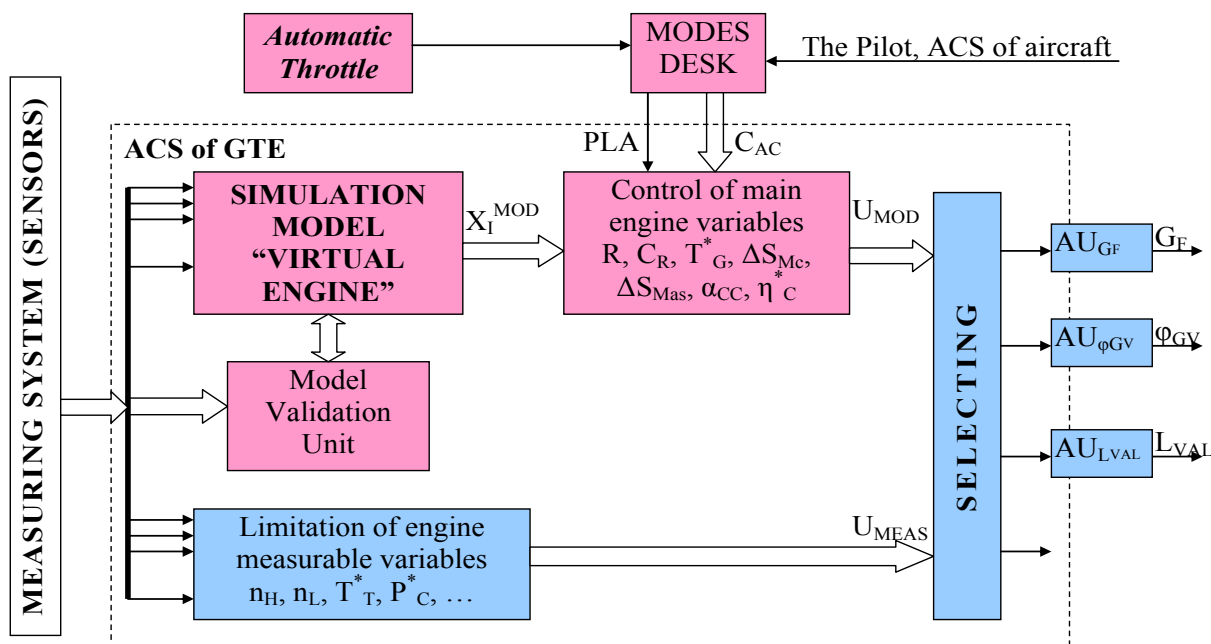


Fig. 1. Block-diagram of automatic control system of TFE with OESM

With similar to structural construction of control loops used in modern digital automatic control system, the considered system additionally contains OESM with its validation algorithms, as well as "virtual" control loops and the limiters differing from "real" in that, engine variables calculated by OESM are used in these loops instead of measured.

Further, let's consider one of the probable control laws complexes of the modern TFE which may be used in "virtual" and "real" controllers of a control system with high level OESM.

## 2. TFE control laws with OESM as a part of the control system

The block diagram of a part of the control system with controllers affecting on fuel flow  $G_F$  in CC is shown in fig. 2.

The block-diagram presents onboard engine simulation model, integrated into the control system with its validation algorithms, controls scheduling unit which deals with variables calculated by onboard model and limits scheduling unit which deals with measurable variables. Preset values  $X_i^{SET}$  of controlled variables are formed in units. Differences between  $\Delta X_i = X_i^{SET} - X_i^{MOD}$  and  $\Delta X_i = X_i^{SET} - X_i^{MEAS}$  determined from calculated  $X_i^{MOD}$  and measured  $X_i^{MEAS}$  are selected after

conversion under the condition of minimum (schedules at steady modes and during acceleration) or maximum (schedules during deceleration) demand of the fuel flow through the use of typical control laws.  $U_{GF}$  is an output signal of selected control channel at present sampling time, which acts on fuel metering unit.

At *steady* modes, main engine schedules use variables, calculated in the OESM:

$$\begin{aligned} R &= f(PLA, T^*_b, P^*_b, C_{ACi}), \\ C_{RMAX} &= f(PLA, T^*_b, P^*_b, C_{ACi}), \\ T^*_{GMAX} &= f(PLA, T^*_b, P^*_b, C_{ACi}), \end{aligned}$$

where  $C_{ACi}$  – signals from aircraft systems.

These schedules act on main fuel flow by selection of minimum value, so that to provide the index value of engine thrust  $R$  on all its operating conditions under the maximum value of specific fuel consumption  $C_R$  limitation at cruise conditions and maximum temperature of gas  $T^*_G$  before a HPT limitation at full power conditions of the TFE.

At *transient* modes, the schedules providing a change of engine thrust rate that is necessary for current flying task under the limitation of variables which influence on engine fail-safety, engine lifetime and operating effect of major engine units are applied in addition.

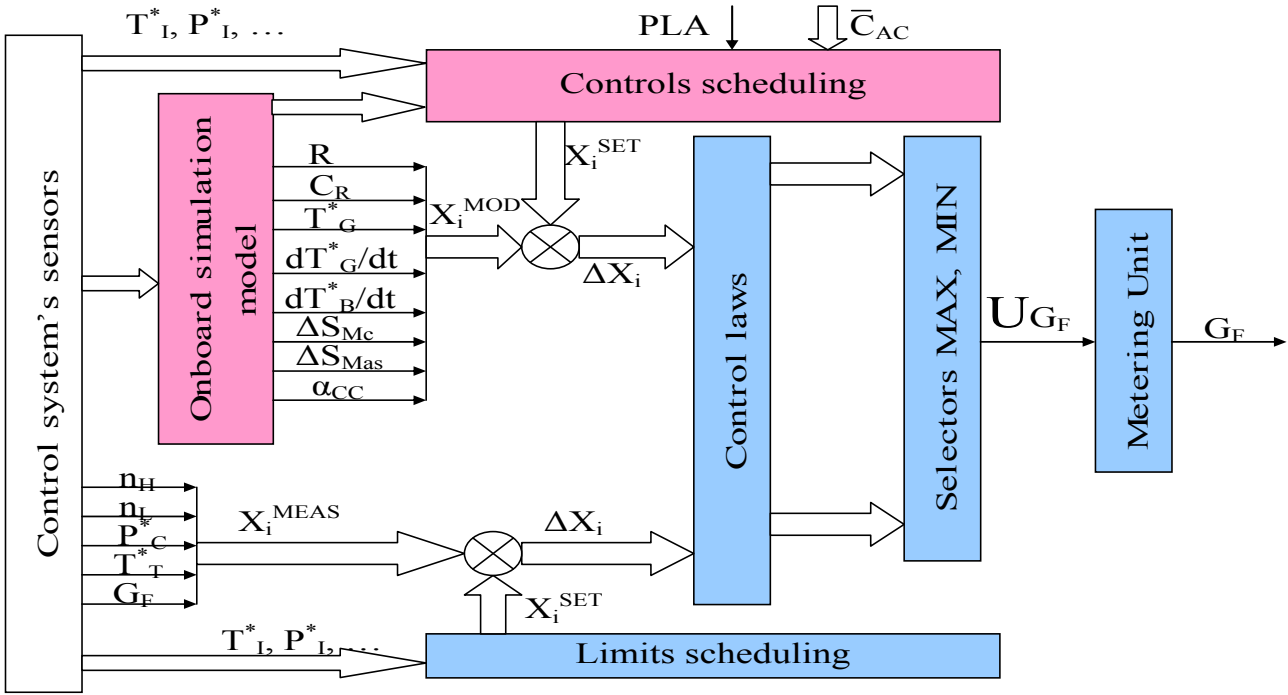


Fig. 2. The block-diagram of the major loop

During acceleration:

$$R_{ACC} = f(t, C_{ACi}),$$

$$\Delta S_{MHPC\ cons} = f(n_{H\ CORR}),$$

$$dT_G^*/dt = f(n_{H\ CORR}).$$

During deceleration:

$$R_{DEC} = f(t, C_{ACi}),$$

$$\Delta S_{MLPC\ cons} = f(n_{L\ CORR}),$$

$$\Delta S_{MAS\ cons} = f(n_{AS\ CORR}),$$

$$\alpha_{CC} \leq \alpha_{CC\ MAX},$$

where  $n_{H\ CORR}$  – rotation speed of high-pressure rotor, corrected by design input temperature of HPC,

$n_{AS\ NORM}$  – rotation speed of low-pressure rotor, corrected by design input temperature of AS,

$\Delta S_{MHPC\ spent}$  – spent stall margin of HPC during acceleration,

$\Delta S_{MLPC\ spent}$ ,  $\Delta S_{MAS\ spent}$  – spent stall margin of LPC and AS during deceleration.

Schedules based on measurable variables employ some limits to improve engine reliability together with protect against stall margin disturbance and engine disintegration:

$$n_L = f(PLA, T_I^*, C_{ACi}),$$

$$n_{H\ MAX} = f(T_I^*),$$

$$P_{C\ MAX}^* = const,$$

$$T_{T\ MAX}^* = f_T(T_I^*),$$

$$(G_F/P_C^*)_{ACC} = f_{G\ acc}(n_{H\ CORR}^1),$$

$$(G_F/P_C^*)_{DEC} = f_{G\ dec}(n_{H\ CORR}^1),$$

where  $n_{H\ CORR}^1$  – rotation speed of HPR, corrected by measured inlet temperature  $T_I^*$ .

The block-diagram of HPC guide vanes controller is shown in **fig. 3**. There are schedules which control variables counted by OESM and measured variables of the engine cycle.

The schedules providing the maximum HPC efficiency value ( $\eta_{HPC\ MAX}^*$ ) under the limitation of the minimum stall margin value ( $\Delta S_{MHPC\ MIN}$ ) are the major.

Optimum change of these variables for specific HPC may be implemented, for example, by the schedules in the form of

$$\pi^* C/G_{C\ NORM} = f(n_{H\ CORR}) \text{ and}$$

$$\eta_{HPC}^* = f(n_{H\ CORR}, \pi^* C).$$

The block-diagram in **fig. 4** demonstrates control loops of air bleed valve from HPC for turbines cooling.

Change in consumption of the air bleed for turbines cooling may be done depending on design value of the gas temperature at the appropriate turbine input, for example:

$$L_{VAL\ HPT} = f(T_G^*),$$

$$L_{VAL\ LPT} = f(T_{1LPT}^*),$$

where  $L_{VAL\ HPT}$ ,  $L_{VAL\ LPT}$  - positions of air bleed valves for HPT and LPT cooling.

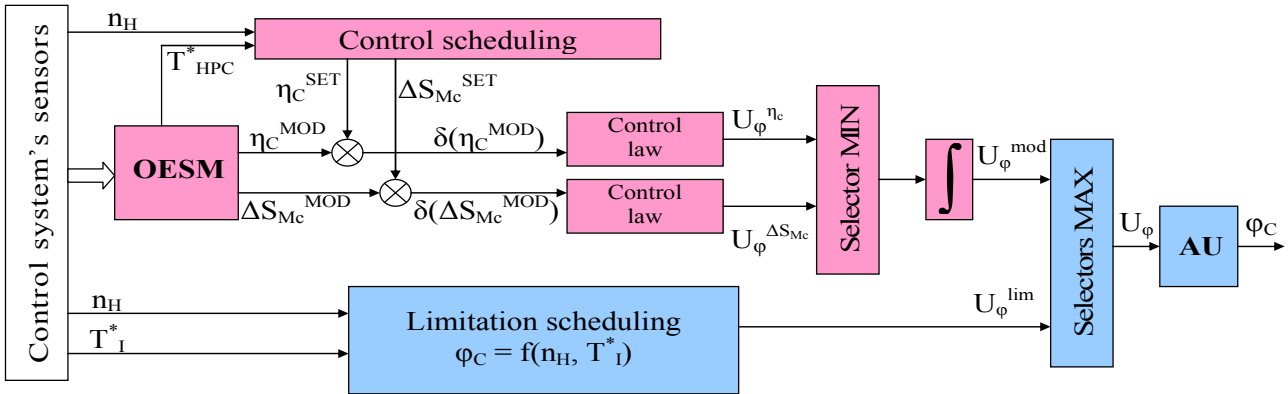


Fig. 3. The block-diagram of a  $\varphi_{GV}$  HPC control loop

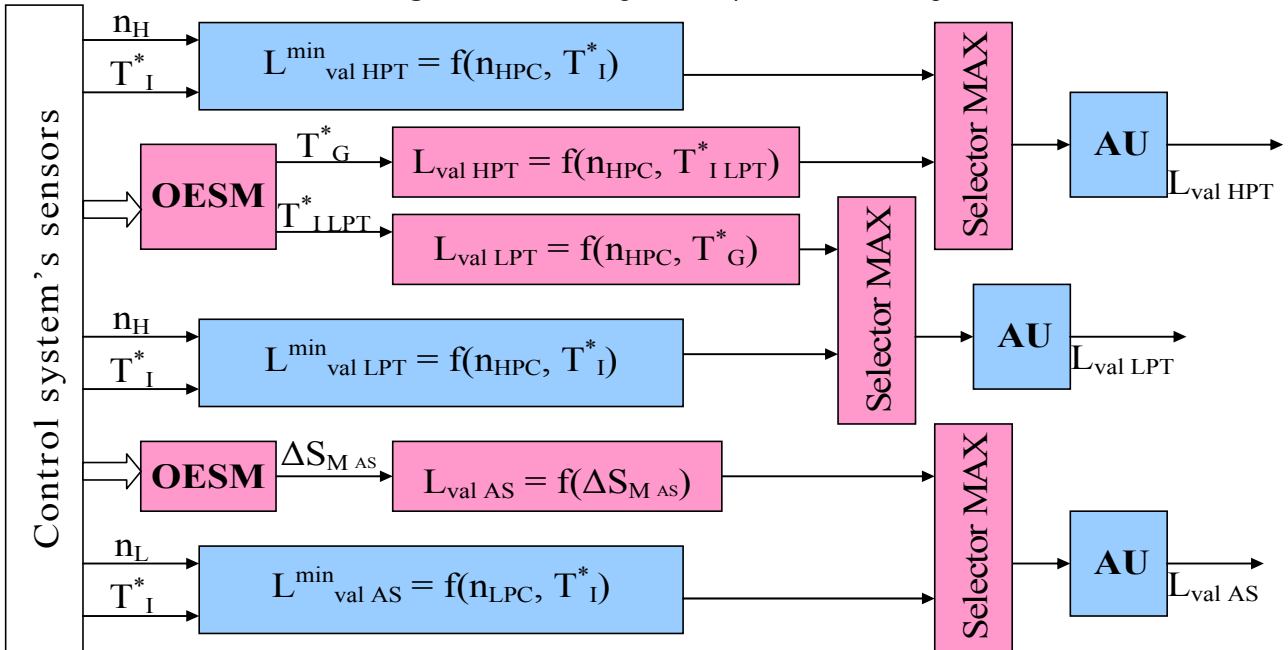


Fig. 4. The block-diagram of bleed valves  $L_{VALi}$  control loop.

The block-diagram of a control loop which acts air-bleed valve from AS is shown in **fig. 4**.

Because air bleed from AS is carried out for the conservation of stall margin of LPC add stage, its value (air bleed valve position  $L_{VAL AS}$ ) can varies with the value of stall margin of AS (actual or spent) calculated in the OESM:

$$L_{VAL AS} = f(\Delta S_{MAS}).$$

Guard controllers of mechanization elements in the engine flow channel work under schedules:

$$\varphi_{GVHPC} = f_{\varphi}(n_{H CORR}^I),$$

$$L_{VAL I} = f_{Li}(n_{H CORR}^I).$$

Hereafter, controllers realizing calculated variables schedules, shall be designated as virtual, and controllers of measured variables – real.

### 3. Evaluation of TFE control efficiency with the use of unmeasurable variables

This section describes some evaluation results of unmeasurable variables control by OESM in respect of major loop, exposing on main fuel flow.

The structure of a major loop of control system (**fig. 2**) with "virtual" and "real" control loops and control schedules on calculated and measured variables, considered in section 2, have been actualized in integrated simulation model «Engine – Control System». The model of engine PD-14 type, developed on the base of the engine components performances provided by Aviadvigatel OJSC, has been implemented as engine in the integrated model.

At the first stage, calculations of processes in the engine have been carried out under the accepted PD-14 control schedules for measured variables. Schedules for unmeasurable variables based on calculation data have been set, so that with the accepted rated performances of engine components, variables of engine cycle at steady and transient modes are the same while engine controlling on measured and calculated variables.

In **fig. 5** there are calculation data of engine variables, obtained in application of control schedules accepted for PD-14 engine, at throttle modes with rated performance of its components, as well as, with using instead of the basic schedule

$$n_L = f(PLA, T_b^*, P_b^*, C_{ACi}),$$

control schedule in the form of:

$$R = f(PLA, T_b^*, P_b^*, C_{ACi}),$$

which provides preset engine thrust by means of a "virtual" control loop containing onboard engine model. Thrust maintenance schedule is chosen in such a manner as to provide a demanded thrust at Idle and MAX power modes as well as its linear dependence on PLA at intermediate modes.

Diagrams in **fig. 5** indicate that in this case, the changes of engine variables along a throttle line are almost the same.

There are keys in **fig. 5** and further:

TIME, s – time;

$G_F$ , kg/s – main engine fuel flow;

R – an engine thrust;

CR – specific fuel consumption;

N2OT – corrected relative value of HPC rotation speed;

N21OT – relative value of HPC rotation speed corrected by temperature  $T_1^*$ ;

AL – air ratio in CC;

GTPK – the ratio between main burner fuel flow and air pressure behind HPC;

DKY\_sp – the value of spent HPC stall margin.

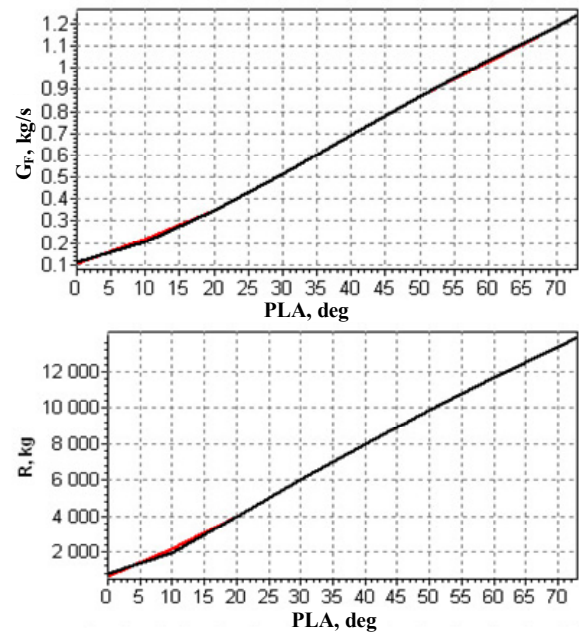


**Fig. 5.** Variation of TFE variables at throttle modes ( $M=0, H=0$ ) with rated performances of engine components

- control schedule  $n_L = f(PLA, T_b^*, P_b^*, C_{ACi})$
- control schedule  $R = f(PLA, T_b^*, P_b^*, C_{ACi})$

In **fig. 6** there are calculation data under the deviation of engine performances from its rating values. In this case, air pressure recovery ratio in bypass duct  $\sigma_{HK}$  is reduced by 2 %.

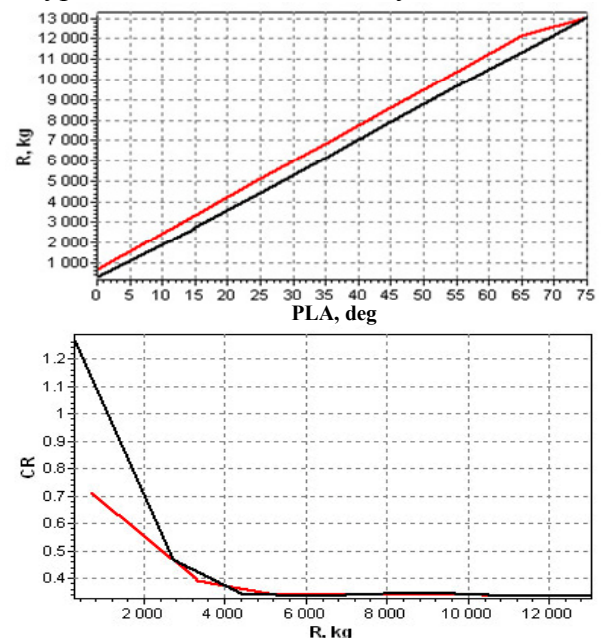


**Fig. 6.** Variation of TFE variables at throttle modes ( $M=0, H=0$ ),  $\sigma_{BD} = 0.98\sigma_{BD\text{RATE}}$

- control schedule  $n_L = f(PLA, T_b^*, P_b^*, C_{ACi})$
- control schedule  $R = f(PLA, T_b^*, P_b^*, C_{ACi})$

It is evident, that in this case, when the schedule  $n_L = f(PLA, T_b^*, P_b^*, C_{ACi})$  is main, at part power modes the thrust essentially

decreases (by 500...700kg). Under application of the schedule  $R = f(PLA, T_b^*, P_b^*, C_{ACi})$  thrust set values are kept constant up to achievement of the maximum rotation speed  $n_L$ .

It is visible also that in this case values of the specific fuel consumption  $C_R$  are smaller at low power settings.

Farther, let's consider some results of performance evaluation when calculated variables of TFE are controlled in transient modes.

The calculation data of engine variables in the context of rated performances of its components during acceleration are shown in **fig. 7**. Processes are obtained in application of control schedules accepted for PD-14 engine, and in using the schedule like this:

$$\Delta S_{MHPC\ cons} = f(n_{H\ CORR}),$$

which provides the limitation of maximum value of spent HPC stall margin  $\Delta S_{MHPC\ cons}$  using "virtual" control loop with onboard engine model, instead of the fuel flow limiting during acceleration which is of the form:

$$(G_F/P^*_C) = f_{G\ acc}(n_H, T^*_I),$$

The schedule  $\Delta S_{MHPC\ cons} = f(n_{H\ CORR})$  is implemented in the form of

$$\Delta S_{MHPC\ cons} < 17\%,$$

That provides change of HPC stall margin during acceleration close to obtained on application of the rated fuel flow limitation.

In **fig. 8...11** there are calculation data of acceleration processes, obtained at a deviation of engine and control system performances from its rated values. "Real" and "virtual" control schedules are the same as for processes in **fig. 7**.

In **fig. 8, 9** there are acceleration processes, obtained under the deviation of value of pressure recovery ratio in CC by  $\pm 3\%$  of design, and in **fig. 10, 11** – under the deviation by  $\pm 5\%$  of value of HPC rotation speed  $n_{C\ CORR\ VAL}$  at wich HPC air bleed valve shuts. Processes in **fig. 8, 10** are obtained under the limitation of fuel flow limitation during acceleration process with the schedule

$$(G_F/P^*_C) = f_{G\ acc}(n_H, T^*_I),$$

and processes in **fig. 9, 11** – under the "virtual" limitation of spent HPC stall margin with the schedule

$$\Delta S_{MHPC\ cons} < 17\%.$$

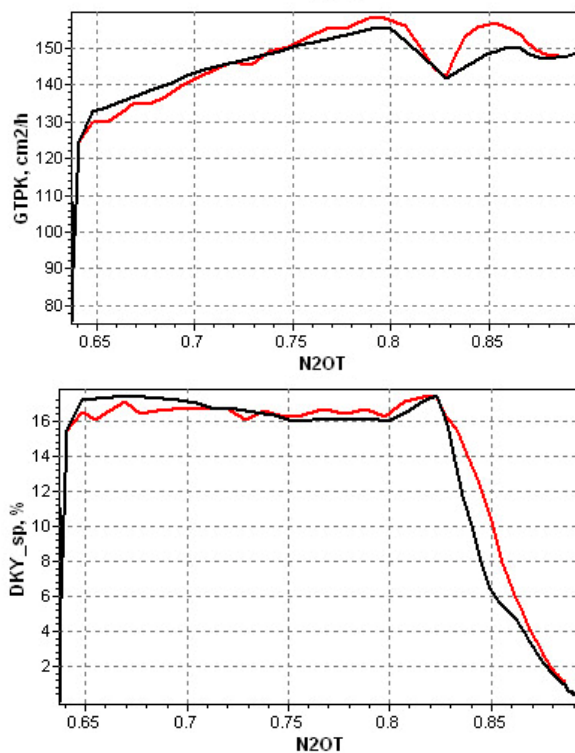


**Fig. 7.** Acceleration at  $M = 0, H = 0$  with rated performances of engine components

— limitation  $G_F$  by the schedule  $(G_F/P^*_C) = f_{G\ acc}(n_H, T^*_I)$ ,  
 — «virtual» limiter  $\Delta S_{MHPC\ cons} < 17\%$ .

Diagrams show that under such typical deviations from accepted rated performances of TFE and its control system and under the limitation of the main fuel flow by the schedule  $(G_F/P^*_C) = f_{G\ acc}(n_H, T^*_I)$ , a 3...6% increase (20...30% of rated value) of spent HPC stall margin is possible. Application of  $\Delta S_{MHPC}$  "virtual" limitation by onboard model allows providing required stall margin under the various deviations of TFE performances and actuating units of control system.

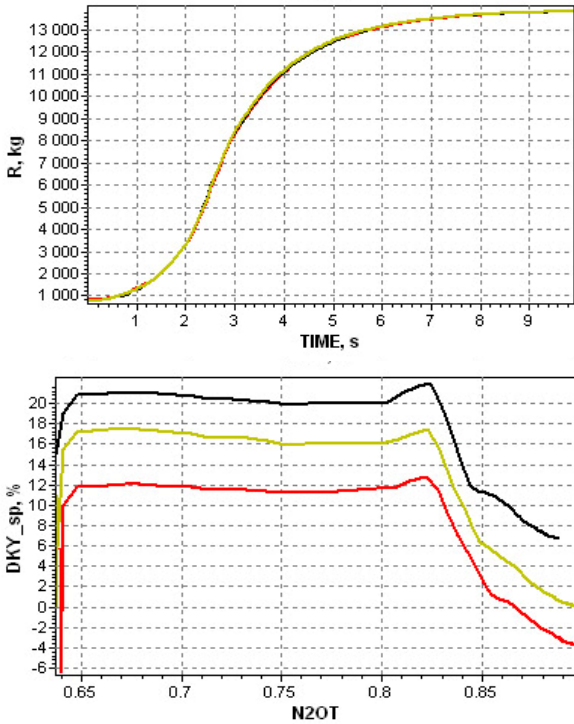


**Fig. 8.** Acceleration at  $M = 0$ ,  $H = 0$  with various values of  $\sigma_{CC}$  and  $G_F$  limitation under the schedule  $(G_F/P^*C) = f_{G acc}(n_H, T^*_I)$

— rate  $\sigma_{CC}$   
 —  $\sigma_{CC} = 0.97 \sigma_{CC rate}$   
 —  $\sigma_{CC} = 1.03 \sigma_{CC rate}$

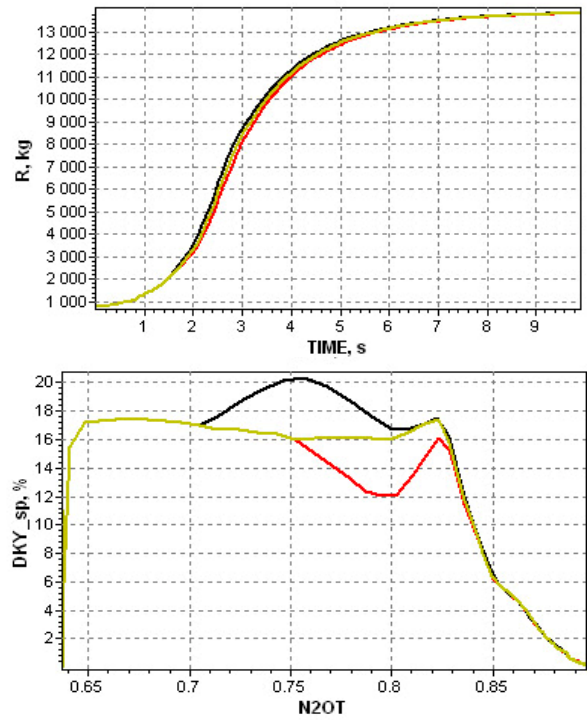


**Fig. 10.** Acceleration at  $M = 0$ ,  $H = 0$  with various values of  $n_{C rate VAL}$  and  $G_F$  limitation under the schedule  $(G_F/P^*C) = f_{G acc}(n_H, T^*_I)$

—  $n_{C rate VAL} = 75\%$  (rated value)  
 —  $n_{C rate VAL} = 70\%$   
 —  $n_{C rate VAL} = 80\%$

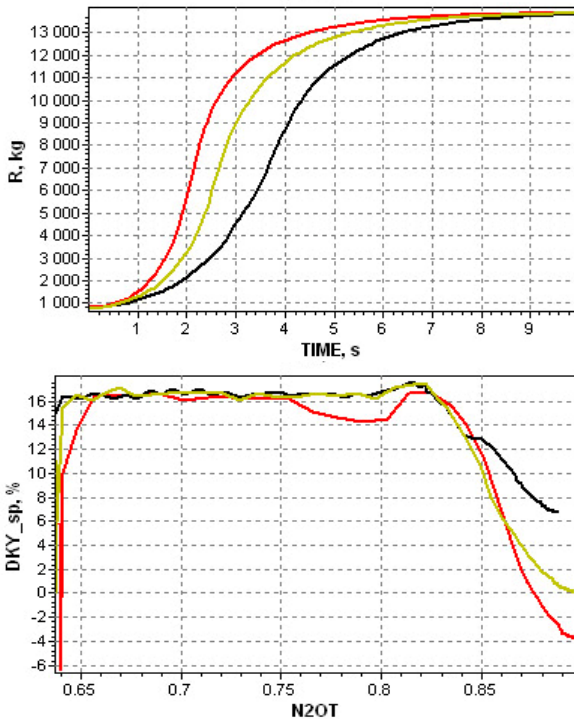


**Fig. 9.** Acceleration at  $M = 0$ ,  $H = 0$  in application of "virtual" limitation  $\Delta S_{M HPC spent} \leq 17\%$  with various values of  $\sigma_{CC}$

— rate  $\sigma_{CC}$   
 —  $\sigma_{CC} = 0.97 \sigma_{CC rate}$   
 —  $\sigma_{CC} = 1.03 \sigma_{CC rate}$

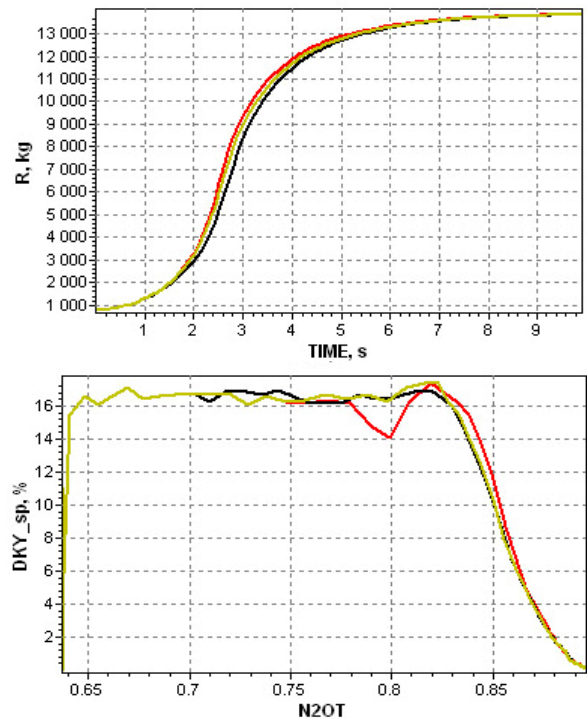


**Fig. 11.** Acceleration at  $M = 0$ ,  $H = 0$  with various values of  $n_{C rate VAL}$  and in application of "virtual" limitation  $\Delta S_{M HPC spent} \leq 17\%$ .

—  $n_{C rate VAL} = 75\%$  (rated value)  
 —  $n_{C rate VAL} = 70\%$   
 —  $n_{C rate VAL} = 80\%$

In **fig. 12** and **fig. 13** there are results of control performance evaluation by the example of deceleration, when calculated by onboard model TFE variables are controlled. The processes shown in **fig 12** are obtained from two ways of control: in application of the regular limitation of the fuel flow during deceleration in the form of  $(G_F/P^*_C) = f_{G dec}(n_H, T^*_I)$  and "virtual" limitation of air-to-fuel ratio in CC  $\alpha_{CC}$  calculated by OESM. The limitation of  $\alpha_{CC}$  is set such that with rating data of engine components, deceleration processes are similar to the processes obtained in application of regular limitation of the fuel flow.

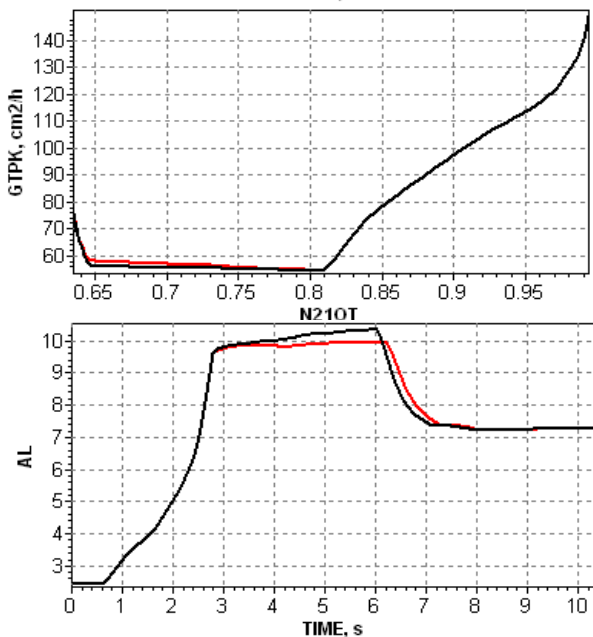


**Fig. 12.** Deceleration at  $M = 0, H = 0$  with rated performances

—  $G_F$  limitation by the schedule  $(G_F/P^*_C) = f_{G dec}(n_H, T^*_I)$  at  $\delta_{G_F/P^*_C} = 0$   
 — "virtual" limitation  $\alpha_{CC} \leq 10$

Processes in **fig. 13**, appropriating to limitation of the fuel flow during deceleration are obtained through introduce a -5 % total error ( $\delta_{G_F/P^*_C}$ ) in measurement of  $G_F/P^*_C$  complex. Diagrams show that with such errors in measurement of the fuel mass flow and limitation of the main fuel flow by the schedule  $(G_F/P^*_C) = f_{G dec}(n_H, T^*_I)$ , air-fuel-ratio in CC  $\alpha_{CC}$  may raise to critical values, whereby flameout in CC is possible. The use of "virtual" limitation of the maximum  $\alpha_{CC}$  value by means of onboard model allows to improve the maintenance of steady-state burning the CC.

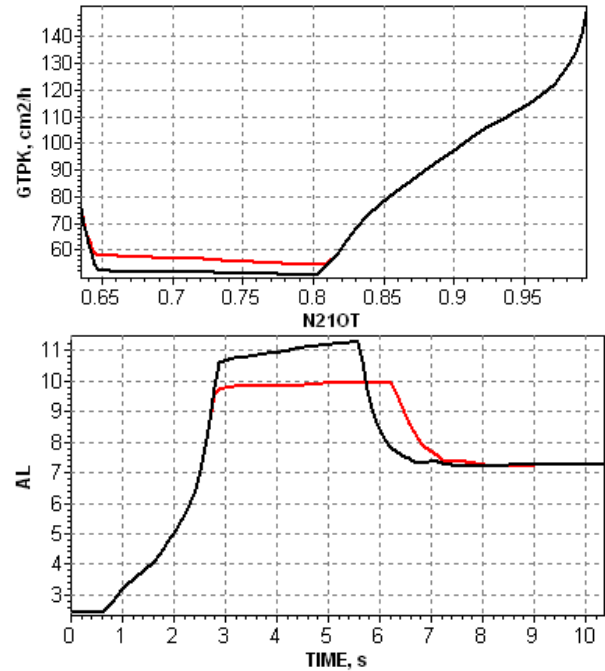


**Fig. 13.** Deceleration at  $M = 0, H = 0$  with  $\delta_{G_F/P^*_C} = -5\%$   
 —  $G_F$  limitation by the schedule  $(G_F/P^*_C) = f_{G dec}(n_H, T^*_I)$ ,  
 — "virtual" limitation  $\alpha_{CC} \leq 10$

Finally, we give an example of possible engine performances upgrade, when onboard model is being applied in control loops of mechanization elements in the engine flow channel.

It is well-known that in modern TFE air for turbines cooling is bled from the compressor. Also, the value of bleed air is controlled by special valve in such a way that at reduced power conditions it is approximately twice as little than at maximum rating. It is done by change of valve position when achieving the set value of compressor rotation speed  $n^1_{C CORR}$ , corrected by an input engine temperature  $T^*_I$ . Significantly more objective indicator of the required value of air bleeding for turbines cooling is the turbine inlet temperature  $T^*_{G HPT}$  and  $T^*_{G LPT}$  respectively. Unmeasurable in modern control systems values  $T^*_{G HPT}$  and  $T^*_{G LPT}$  can be calculated by high level OESM in hand.

Let us consider operational effect of such control method in respect to the air bleed valve for turbines cooling. When  $n^1_{C CORR}$  reaches the value equal to 85 %, the air bleed becomes increased (reduced). At engine steady conditions it corresponds to  $T^*_{G HPT}$  and  $T^*_{G LPT}$  whose values are about 1200K and 830K.

During acceleration, air bleeding for turbines cooling is expanded when the value of  $n^1_{C\text{CORR}}$  equal 85 % is reached, it corresponds to higher values of gas temperature  $T^*_{G\text{HPT}}$  and  $T^*_{G\text{LPT}}$  (about 1550 and 1100K), that can lead to increase in temperature of turbines blade and engine lifetime loss due to their low-cycle fatigue. When air bleed valve control applying, the valve changes position by temperature  $T^*_{G\text{HPT}}$  counted by OESM, so values of temperatures  $T^*_{G\text{HPT}}$  and  $T^*_{G\text{LPT}}$  at which turbines cooling rate increases, are almost similar to their values at steady modes. Thus, as is evident from **fig. 14**, the maximum rate of blade temperature rise decreases.

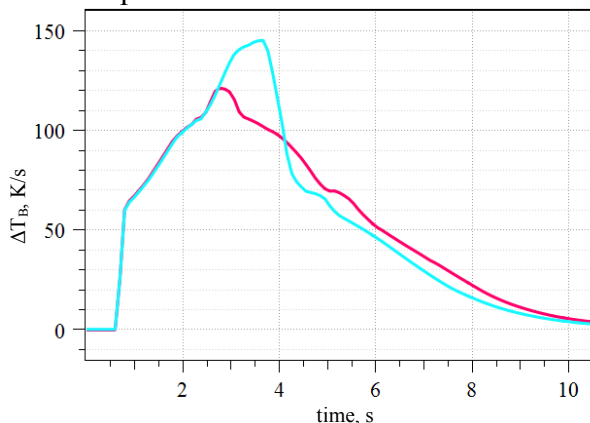


**Fig. 14.** Rate of HPT blades temperature change during acceleration

— Control of bleed valve for HPT cooling by rotation speed  $n^1_{C\text{CORR}}$ ,  
 — Control of bleed valve for HPT cooling by temperature  $T^*_{G\text{HPT}}$

“Virtual engine” software created on the base of models like those has been implemented in object modules which were meant for uploading to GTE control system. That sort of object module has been implemented in microcontroller **TE-STM32F103** (core ARM Cortex-M3; **fig. 15**). Procedure of communication between calculation program unit and control system with interval of 28 ms when 4 solving cycles of model equations are carried out has also been actualized. It was found that the size of the program load module into microcontroller flash-memory is 54196 bytes, and wall time of all model equations at one integration step is about two times less than the real time.

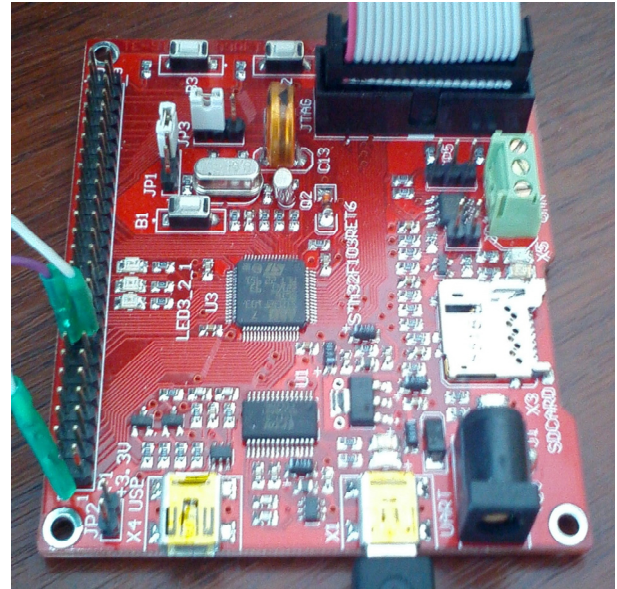


**Fig. 15.** OESM implementation in microcontroller

## Conclusions

Control strategy and design concept of TFE control system by means of the software «virtual engine», based on all-speed real-time engine thermogasdynamical simulation model, were formulated.

The algorithmic software of a control system containing onboard engine simulation model, as well as "virtual" loops controlling variables calculated by onboard model have been developed. Methods of OESM validation while in operation on a running engine have been developed too.

Evaluation of unmeasurable variables control efficiency by means of OESM has been done in respect to turbofan engine.

## References

- [1] Michael V. Nathal. *Intelligent Propulsion System Foundation Technology Summary of Research*. The Ohio State University Research Foundation. National Aeronautics and Space Administration Glenn Research Center. June 2008.
- [2] F.D. Golberg, O.S. Gurevich, A.A. Petukhov. *On-board simulation model as part of GTE control system for improving fault tolerance and control quality*. Automatic control systems of gas-turbine engines /Under the editorship of O.S. Gurevich – M.: TORUS PRESS, 2010. – 264 pp.

### **Contact Author Email Address**

mailto: fegolb@ciam.ru

### **Copyright Statement**

The authors confirm that they, and/or their company or organization, hold copyright on all of the original material included in this paper. The authors also confirm that they have obtained permission, from the copyright holder of any third party material included in this paper, to publish it as part of their paper. The authors confirm that they give permission, or have obtained permission from the copyright holder of this paper, for the publication and distribution of this paper as part of the ICAS 2014 proceedings or as individual off-prints from the proceedings.